Modeling Supermarket Refrigeration Systems for Supervisory Control in Smart Grid

Shafiei, Seyed Ehsan; Rasmussen, Henrik; Stoustrup, Jakob

Published in:
American Control Conference (ACC), 2013

Publication date:
2013

Document Version
Early version, also known as pre-print

Modeling Supermarket Refrigeration Systems for Supervisory Control in Smart Grid*

Seyed Ehsan Shafiei, Henrik Rasmussen and Jakob Stoustrup

***Abstract*— A modular modeling approach of supermarket refrigeration systems (SRS) which is appropriate for smart grid control purposes is presented in this paper. Modeling and identification are performed by just knowing the system configuration and measured data disregarding the physical details. So, this approach is extendable to different configurations with different modules. The focus of the work is on estimating the power consumption of the system while estimating the display case temperatures as well. This model can however be employed as a simulation benchmark to develop control methods for SRS regarding their power/energy consumptions in the future smart grids. Moreover, the developed model is validated by real data collected from a supermarket in Denmark. The utilization of the produced model is also illustrated by a simple simulation example.**

I. INTRODUCTION

Supermarket refrigeration systems can take part in energy balancing of the grid as intelligent consumers in the smart grid concept by employing the thermal capacity existing in the refrigerated foodstuffs. Since such systems are large scale and developing control methods takes a lot of time for implementations due to large time constants, this motivates us to develop a model that can be used as a simulation benchmark.

There are however a few works in modeling of refrigeration systems for control purposes. In [1] two different models are introduced: a static model considering refrigeration cycle in steady-state to develop set-point optimizing control, and a dynamic model (neglecting condenser module) to design and analysis of desynchronizing control. Although these models are appropriate for a simple refrigeration cycle, they are not directly applicable for a multi-display case system. A comprehensive dynamic modeling is performed in [2] for vapor compression systems; but the model is too detailed and complicated and also the compressor power consumption is not estimated. The steady-state model introduced in [3] is just for optimization of the system coefficient of performance (COP) and does not explain the dynamical behavior of the system.

From smart grid point of view, an appropriate model is introduced in [4] for optimizing the energy consumption of refrigeration systems. Although this model can be employed for a single evaporator system, it cannot model a supermarket refrigeration systems including several display cases. The main problem is that in a single vapor compression cycle it is possible to change the cold reservoir temperature by changing the suction pressure while, on the other hand, in SRS, the display cases temperatures are regulated by controlling the expansion valve and the suction pressure should be regulated to a set-point that can optimize the system performance e.g. COP.

In this paper, a model for supermarket refrigeration systems is developed to be employed as a simulation benchmark in the system architecture shown in Fig. 1. The modeled system can receive the temperature set-points for display cases from a supervisory controller and regulate them by simple hysteresis controllers affect on expansion valves and then estimate the power consumption of the compressor bank for the current operating condition. The modeling is performed by a modular approach in which the system is separated into different subsystems and each subsystem is modeled independently and validated by real data used for identification. This modular method leaves open the possibility of modeling refrigeration systems with different configurations existing in various supermarkets.

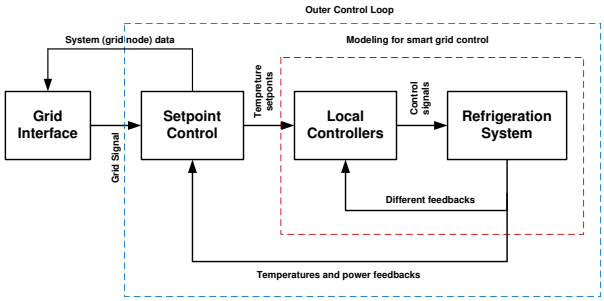

Fig. 1. A typical control system structure for connecting supermarket refrigeration systems to the smart grid

Moreover, the complete system model made by integrating modeled subsystems into a booster configuration is validated by both identification and validation data which shows a satisfactory modeling suitable for the proposed smart grid control structure. Finally, a simple example is provided to show how the developed model can be utilized as a simulation benchmark to implement smart grid control algorithms.

II. SYSTEM DESCRIPTION

Our case study is a CO_2 refrigeration system with a booster configuration shown in Fig. 2 operating in the subcritical cycle. The highest pressure zone starts from the outlet of high stage compressor rack (COMP_HI). Then the gas phase refrigerant enters the gas cooler or condenser to

*This work is supported by the Southern Denmark Growth Forum and the European Regional Development Fund under the Project Smart & Cool.

Authors are with Section for Automation and Control, Department of Electronic Systems, Aalborg University, Aalborg, Denmark {ses, hr, jakob} at es.aau.dk

deliver the absorbed heat to the surrounding. At the outlet of the high pressure control valve (CV_HP), the pressure drops to an intermediate level and the refrigerant which is now in two-phase (mix of liquid and vapor) flows into the receiver (REC). The receiver is to split out the two-phase refrigerant into saturated gas, bypassed by BPV, and saturated liquid flows into expansion valves where the refrigerant pressure drops again. The expansion valves TEV_MT and TEV_LT are driven by hysteresis ON/OFF controllers to regulate the temperature of the fridge display cases and freezing rooms, respectively. Flowing through medium and low temperature evaporators (EVAP_MT and EVAP_LT), the refrigerant absorbs heat from the cold reservoir while a superheat controller also operates on the valves to make sure the refrigerant leaving the evaporators toward compressors is only in the gas phase.

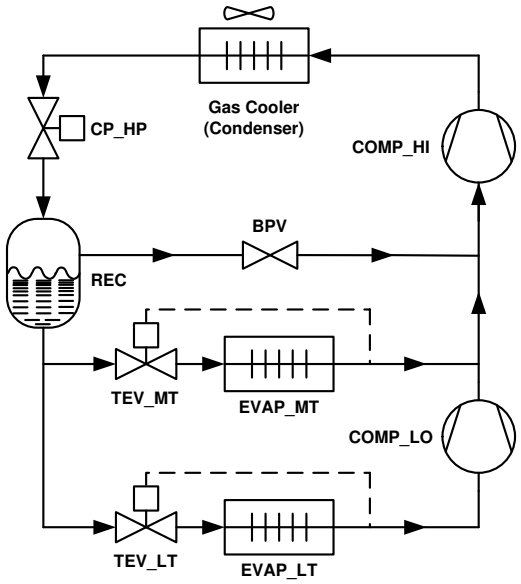

Fig. 2. A typical booster configuration for CO_2 refrigeration systems

III. MODELING

There are three subsystems to be modeled including *display cases*, *suction manifold* including high stage compressor, and *condenser*. The modeling of low temperature section is similar to the medium temperature, so omitted here. The operation of the high pressure valve and the receiver are not modeled since the intermediate pressure at the outlet of receiver is assumed constant.

A. Display Cases

In display cases, heat is transfered from food stuffs to evaporator, $\dot{Q}_{foods/dc}$, and then from evaporator to circulated refrigerant, $\dot{Q}_e$, which is also known as cooling capacity. There is however heat load from supermarket indoor, $\dot{Q}_{load}$, considered as a variable disturbance. Here, we consider the measured air temperature at the evaporator outlet as the display case temperature, T_{dc}. Assuming a lumped temperature model, the following dynamical equations are derived based on energy balances for mentioned heat transfers.

$$MCp_{foods}\frac{dT_{foods}}{dt} = -\dot{Q}_{foods/dc} \tag{1}$$

$$MCp_{dc}\frac{dT_{dc}}{dt} = \dot{Q}_{load} + \dot{Q}_{foods/dc} - \dot{Q}_e \tag{2}$$

where MCp denotes the corresponding mass multiplied by the heat capacity. The energy flows are:

$$\dot{Q}_{foods/dc} = UA_{foods/dc}(T_{foods} - T_{dc}) \tag{3}$$

$$\dot{Q}_{load} = UA_{load}(T_{indoor} - T_{dc}) \tag{4}$$

$$\dot{Q}_e = \dot{m}_r(h_{oe} - h_{ie}) \tag{5}$$

where UA is the overall heat transfer coefficient, h_{oe} and h_{ie} are enthalpies at the outlet and inlet of evaporators, and T_{indoor} is the supermarket indoor temperature. The term $\dot{m}_r$ denotes the mass flow of refrigerant into the evaporator which is determined by the opening degree of the expansion valve and described by the following equation:

$$\dot{m}_r = OD\ KvA\sqrt{2\rho_{suc}(P_{rec} - P_{suc})10^5} \tag{6}$$

in which OD stands for the opening degree of valve with value between 0 to 100%, P_{rec} and P_{suc} are receiver and suction manifold pressures in [bar], ρ_{suc} is the density of circulating refrigerant, and KvA denotes a constant characterizing the valve [5].

B. Suction Manifold

Suction manifold is modeled by a dynamical equation with suction pressure as its state and by employing the mass balance as, [6],

$$\frac{dP_{suc}}{dt} = \frac{\dot{m}_{dc} + \dot{m}_{dist} - \dot{V}_{comp}\rho_{suc}}{V_{suc}d\rho_{suc}/dP_{suc}}, \tag{7}$$

where the compressor bank is treated as a big *virtual compressor*, $\dot{m}_{dc}$ is the total mass flow of display cases, $\dot{m}_{dist}$ is the disturbance mass flow including the mass flow from freezing room and bypass valve, and V_{suc} is the volume of the suction manifold. $\dot{V}_{comp}$ is the volume flow out of the suction manifold:

$$\dot{V}_{comp} = f_{comp}\eta_{vol}V_d \tag{8}$$

where f_{comp} is the virtual compressor frequency (total capacity) of the high stage compressor rack in percent, V_d denotes the displacement volume, and η_{vol} is clearance volumetric efficiency approximated by

$$\eta_{vol} = 1 - c((\frac{P_c}{Psuc})^{1/\gamma} - 1) \tag{9}$$

with constant clearance ratio c, and constant adiabatic exponent γ, [7]. P_c is the compressor bank outlet pressure.

The most important part (for this study) in compressor calculations is to calculate power consumption of the compressor bank, $\dot{W}_{comp}$, given by

$$\dot{W}_{comp} = \frac{1}{\eta_{me}}\dot{m}_{ref}(h_{o,comp} - h_{i,comp}) \tag{10}$$

where $\dot{m}_{ref}$ is total mass flow into the suction manifold, and $h_{o,comp}$ and $h_{i,comp}$ are enthalpies at the outlet and inlet of compressor bank and are nonlinear function of the refrigerant pressure and temperature at the calculation point. The constant η_{me} indicates overall mechanical_electrical efficiency considering mechanical friction losses and electrical motor inefficiencies [7]. The enthalpy of refrigerant at inlet of the manifold is bigger than of the evaporator outlet ($h_{i,comp} > h_{oe}$) due to disturbance mass flows. The outlet enthalpy is computed by

$$h_{o,comp} = h_{i,comp} + \frac{1}{\eta_{is}}(h_{o,is} - h_{i,comp}), \tag{11}$$

in which $h_{o,is}$ is the outlet enthalpy when the compression process is isentropic, and η_{is} is the related isentropic efficiency given by [3] neglecting higher order terms.

$$\eta_{is} = c_0 + c_1(f_{comp}/100) + c_2(P_c/P_{suc}) \tag{12}$$

where c_i are constant coefficients.

C. Condenser

Most of the models developed for condenser need physical details like fin and tube dimensions [8], [9], [10] and thus are not directly applicable here since our modeling approach is mainly based on general knowledge about the system. So, neglecting condenser dynamics, the steady-state multi-zone moving boundary model developed in [3] is utilized here with further considerations.

The condenser is supposed to operate in three zones (superheated, two-phase, and subcooled). A pressure drop is assumed to take place across the first zone (superheated) and is given by, [3],

$$\Delta P_c \triangleq P_c - P_{cnd} = \left(\frac{\dot{m}_{ref}}{A_c}\right)\left(\frac{1}{\rho_{cnd}} - \frac{1}{\rho_c}\right) + \Delta P_f \tag{13}$$

where A_c is the cross-sectional area of the condenser, and P_{cnd} and ρ_{cnd} are the pressure and density at the outlet of the superheated zone. The first term at the right hand side of (13) indicates acceleration pressure drop and the last term stands for the frictional pressure drop (ΔP_f) and assumed constant. The rate of heat rejected is described by (14) for superheated (first) and subcooled (third) zones,

$$\dot{Q}_{c,k} = UA_{c,k}\frac{T_{i,k} - T_{o,k}}{\ln\left[\frac{T_{i,k} - T_{outdoor}}{T_{o,k} - T_{outdoor}}\right]}, \quad k = 1,3 \tag{14}$$

and the following for the two-phase (second) zone.

$$\dot{Q}_{c,2} = UA_{c,2}(T_{i,2} - T_{outdoor}) \tag{15}$$

where UA_c is the overall heat transfer coefficient of the corresponding condenser zone, T_i and T_o are the refrigerant temperature at the inlet and outlet of each zone, and $T_{outdoor}$ is the outdoor temperature. Note that the inlet and outlet temperatures of the two-phase zone are the same when the pressure does not change across it.

The heat transfered by refrigerant flow across the kth zone is provided by the following energy balance equation:

$$\dot{Q}_{c,k} = \dot{m}_{ref}(h_{i,k} - h_{o,k}), \quad k = 1,2,3 \tag{16}$$

in which h_i and h_o are enthalpies at the inlet and outlet of the kth zone. Accordingly, the total rate of heat rejected by the condenser would be:

$$\dot{Q}_c = \sum_{k=1}^{3} \dot{Q}_{c,k} \tag{17}$$

IV. PARAMETER ESTIMATION

An off-line identification is performed in this section to estimate constant parameters and coefficients introduced before. The required data are collected by measurements from a supermarket in Denmark. Identification data are selected from an interval during the day time when no defrost cycle takes place.

An iterative prediction-error minimization (PEM) method, implemented in *System Identification Toolbox* of MATLAB, is employed to estimate model parameters [11]. A modular parameter estimation approach is introduced in which the parameters of each subsystem, considered as a *gray-box model*, are identified by providing related input-output pairs from measurement data.

Nonlinear thermophysical properties of the refrigerant (e.g. enthalpies) are calculated by free software package "RefEqns", [12].

1) Display cases estimations: In this subsystem, the model should be able to estimate mass flow and display case temperatures. So the input and output vectors used for estimation are:

$$U_{dc} = \begin{bmatrix} P_{suc} & T_{indoor} & OD_1 & \cdots & OD_7 \end{bmatrix}^T, \tag{18}$$

and

$$Y_{dc} = \begin{bmatrix} \dot{m}_{dc} & T_{dc,1} & \cdots & T_{dc,7} \end{bmatrix}^T. \tag{19}$$

Estimated parameters for total seven display cases are collected in Table I assuming constant superheat $T_{sh} = 5$ [°C], and constants receiver pressure $P_{rec} = 38$ [bar]. Five hours data sampled every minute are used.

TABLE I
DISPLAY CASES ESTIMATED PARAMETERS

D.C. No.	UA_{load}	$UA_{foods/dc}$	MCp_{dc} $\times 10^5$	MCp_{foods} $\times 10^5$	KvA $\times 10^{-6}$
1	56.1	99.5	3.7	21.6	1.38
2	67.6	1.1	6.3	7.4	1.90
3	145.3	190.5	7.2	65.1	2.65
4	65.6	434.2	8.7	57.2	1.68
5	49.8	196.3	8.7	56.2	3.12
6	75.5	59.6	3.5	9.7	1.36
7	22.8	94.9	3.5	3.4	1.47

Estimation results for display case temperatures and overall mass flow from the expansion valves are illustrated in Fig. 3 and Fig. 4, respectively. For a fair comparison, all temperature plots have the same scale. Also the value of modeling errors computed by dividing the maximum absolute error on the maximum amplitude of variation of the measured signal are provided on each plot which shows the best and worst fit for the 5th and 7th display cases, respectively.

In spite of not using too complicated model and relatively large number of estimated parameters (35 parameters), the display case models show satisfactory results.

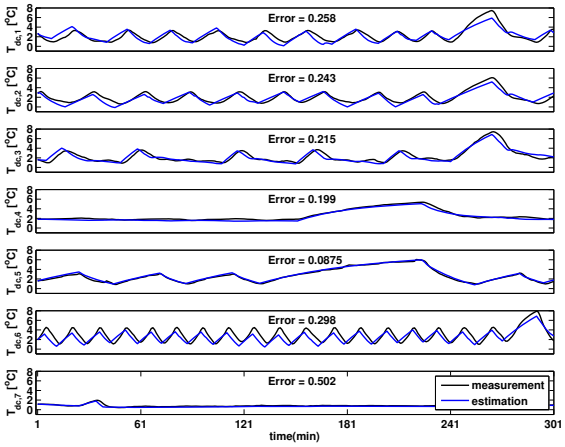

Fig. 3. Estimation of display case temperatures. The 5th display case shows the best fit (error=0.087), and the worst fit is related to 7th one (error=0.502) which is still a good estimation.

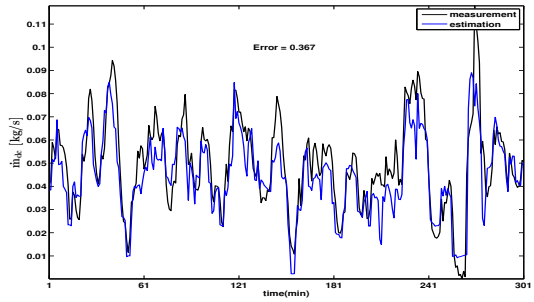

Fig. 4. Estimation of the total mass flow from display cases. It is sum of the mass flows through the expansion valves.

2) Suction manifold estimations: Although the main goal of modeling this section is to estimate power consumption of the compressor bank, we also need to estimate P_{suc} for this purpose as stated in the previous section.

Suction pressure is computed from (7) by entering the following inputs and output into the identification process and assuming $V_{suc} = 2$ and knowing $V_d = (6.5 \times 70/50 + 12.0)/3600$ from compressor label.

$$U_{suc} = \begin{bmatrix} \dot{m}_{dc} & \dot{m}_{dist} & P_c & f_{comp} \end{bmatrix}^T, \quad Y_{suc} = P_{suc} \qquad (20)$$

This results in estimating parameters required for volumetric efficiency in (9) as $c = 0.56$ and $\gamma = 0.52$.

The following inputs and output are chosen to estimate power consumption of the compressor bank.

$$U_{comp} = \begin{bmatrix} P_{suc} & P_c & f_{comp} & \dot{m}_{ref} \end{bmatrix}^T, \quad Y_{comp} = \dot{W}_{comp} \quad (21)$$

The parameters needed for calculating isentropic efficiency are estimated as $c_0 = 1$, $c_1 = -0.52$ and $c_2 = 0.01$, and mechanical-electrical efficiency is also obtained as $\eta_{me} = 0.65$.

Fig. 5 shows estimation results for suction pressure and power consumption. Even though simple first order model introduced for suction manifold cannot generate high frequency parts of the pressure signal, it can fairly estimate a low pass filtered version of the suction pressure. The bottom plot shows a very good estimation of the power consumption.

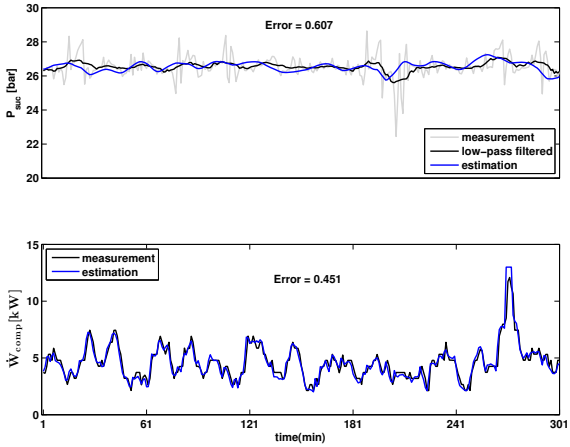

Fig. 5. Suction pressure and power consumption estimations. Suction pressure is regulated at 26 [bar] by local compressor bank controller. Variation of consumption is mainly because of changing mass flow due to hysteresis and superheat control of expansion valves. Mechanical-electrical efficiency is obtained $\eta_{me} = 0.65$.

3) Condenser: In the condenser model, corresponding parameters should be estimated such that the heat transfer generated by the steady-state model has to be equal to the heat transfer delivered by refrigerant mass flow. Input vector used for identification is

$$U_{cnd} = \begin{bmatrix} T_{i,cnd} & \dot{m}_{ref} & T_{outdoor} \end{bmatrix}^T, \qquad (22)$$

where $T_{i,cnd}$ is the refrigerant temperature at the inlet of condenser which is also the inlet of the first zone. Enthalpies $h_{o,1} = h_{i,2}$ and $h_{o,2} = h_{i,3}$ are the enthalpies of saturated vapor and saturated liquid at the pressure P_{cnd}, respectively. The output temperature is also calculated by assuming 2 °C constant subcooling. The desired output to be estimated is

$$Y_{cnd} = P_c \qquad (23)$$

Estimation result is shown in Fig. 6 with the following parameters. The associate result for pressure drop can justify the assumption says it mainly takes place in the first (superheated) condenser zone. Despite considering a simple steady-state model for condenser and also not using any physical detail of it, the estimation is still acceptable

A_c	ΔP_f	$UA_{c,1}$	$UA_{c,2}$	$UA_{c,3}$
0.0073	0.52	332	3185	148

V. SYSTEM INTEGRATION AND MODEL VALIDATION

Thus far, three independent models developed for three different subsystems using corresponding measured inputs and outputs for each. In this section, we integrate all subsystems to build a complete model for supermarket refrigeration systems ready for use as a simulation benchmark.

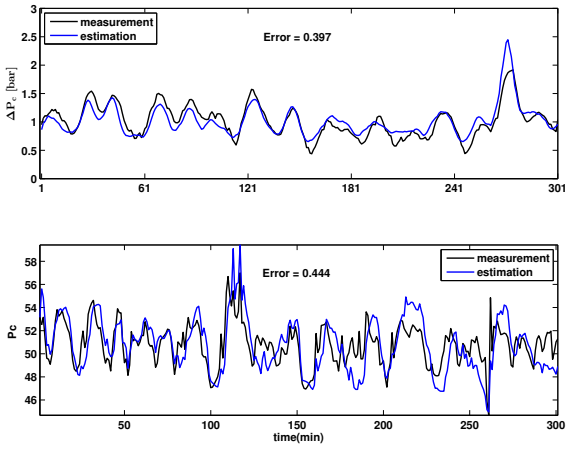

Fig. 6. Estimation of the pressure drop and the pressure at the condenser inlet. In spite of not using any physical detail of the condenser and disregarding dynamics, the estimation results are still acceptable.

The inputs used in running the model are the opening degree of expansion valves (OD_i) and the running capacity of compressor bank (f_{comp}).

$$U_{sys} = \begin{bmatrix} OD_1 & \cdots & OD7 & f_{comp} \end{bmatrix} \tag{24}$$

The disturbance vector is:

$$U_{dist} = \begin{bmatrix} \dot{m}_{dist} & T_{indoor} & T_{outdoor} \end{bmatrix} \tag{25}$$

In order to simulate the control strategy depicted in Fig. 1, the SRS model should be able to estimate display case temperatures and compressor power consumptions with satisfactory degrees of accuracy. Fig. 7 and 8 show the results of running the model by (24) and (25) using the data set used for identification in the previous section.

The estimation errors does not increase significantly and the results are still convincing and can satisfy our expectation to have a model as a simulation benchmark.

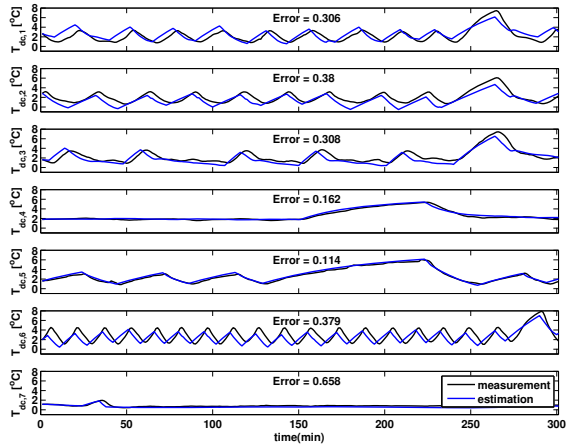

Fig. 7. Estimation of display case temperatures after system integration and using training data. The estimation error a little increases due to modeling error associated with each subsystem.

As mentioned before, the system inputs picked out of a set of data used for identification process (training data). In order to further validate the developed model, the system is run with the same frame of data but for another day and the output results are compared with the related data. As can be seen from Fig. 9 and 10, the model can still well estimate the required display case temperatures and compressor power consumptions with close accuracy as for training data.

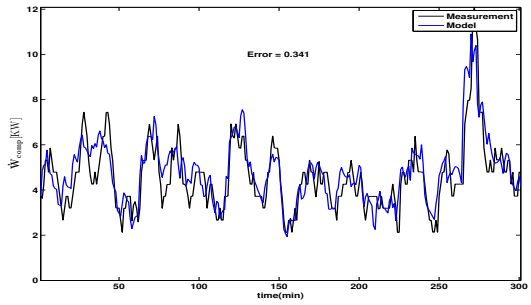

Fig. 8. Power consumption estimation of the compressor bank after system integration and using training data. The estimation is still satisfactory in spite of existing estimation errors associated with each subsystem model.

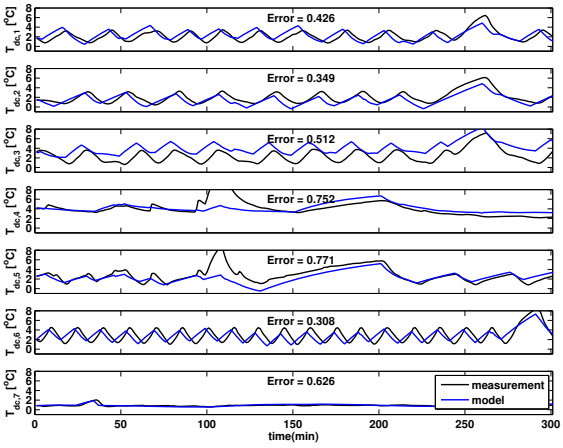

Fig. 9. Estimation of display case temperatures after system integration and using validation data.

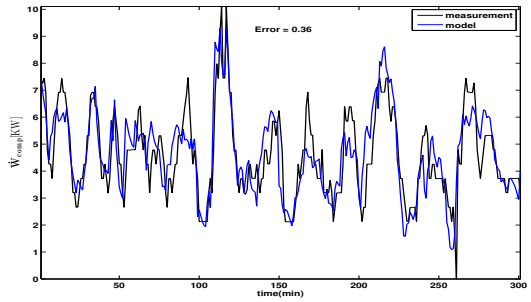

Fig. 10. Power consumption estimation of the compressor bank after system integration and using validation data. The estimation error is close to what using the training data which again indicates the model validation.

VI. APPLICATION EXAMPLE

In direct control of consumers in the smart grid, they should follow the power reference sent by the grid based on their flexibilities. Discussing the flexibilities and other details in this context is however out of scope of this paper. In the following we will show by a simple example that how the

produced model can be utilized in implementing the direct control with the structure shown in Fig. 1.

The supervisory controller includes a PI controller which regulates the power consumption to the reference level received from the grid. The output of the PI controller after scaling by defined gains of set-point change for each display case applied to the refrigeration system model (see Fig. 11).

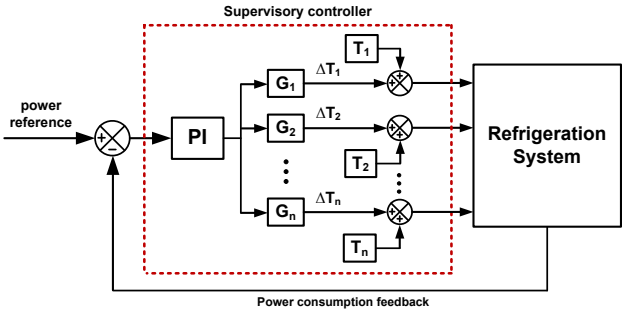

Fig. 11. A simple direct control structure. The controller applies the change of control signal (the temperature set-points here) to the plant.

Fig. 12 shows the power consumption in a normal operation when no supervisory control affects the system on the top, and the related direct control on the bottom. The system is simulated for one day. The 60-minute moving average of the power is shown in the plot. A sinusoidal shape of change in the average consumption in normal operation is because of the sinusoidal change of outdoor temperature.

The control objective is the average power consumption of refrigeration system to follow the power reference while respecting the temperature limits in display cases. The corresponding display case temperatures are also depicted in Fig. 13. This is only a simple example to show the basic idea; the design of advanced controls is left to future works.

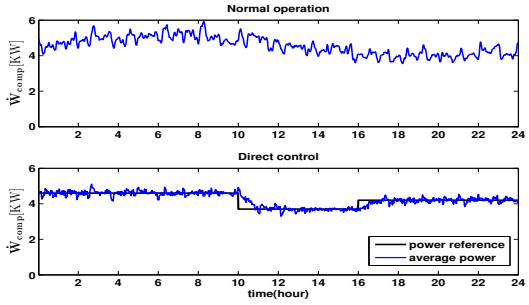

Fig. 12. Power consumption for one day operation. High frequency fluctuations are mainly caused by hysteresis control of display cases. Direct control can successfully follow the reference.

VII. CONCLUSIONS

A supermarket refrigeration system suitable for supervisory control in the smart grid is modeled. The system was divided into three subsystems each modeled and validated independently. The proposed modular modeling approach leaves open the possibility of modeling refrigeration systems with different configurations and operating conditions. Provided results showed the satisfactory modeling. These subsystem models were finally integrated to make a booster

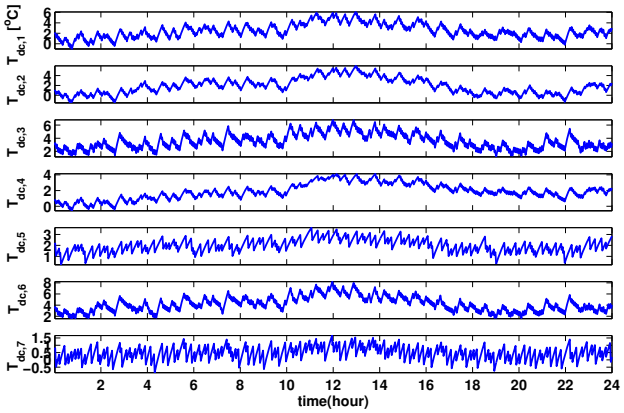

Fig. 13. Display case temperatures are changed by supervisory controller to regulate the consumption.

configuration and the corresponding results confirmed the effectiveness of the proposed modeling approach. At the end, a simple simulation example was provided to show the utilization of the developed model.

VIII. ACKNOWLEDGMENTS

The authors wish to acknowledge Danfoss Refrigeration & Air Conditioning for supporting this research by providing valuable data under the ESO2 research project.

REFERENCES

[1] L. F. S. Larsen, *Model Based Control of Refrigeration Systems*. PhD thesis, Aalborg University, Section of Automation and Control, 2005.

[2] R. Shah, A. Alleyne, C. Bullard, B. Rasmussen, and P. Hrnjak, "Dynamic modeling and control of single and multi-evaporator subcritical vapor compression systems," tech. rep., University of Illinois, Air Conditioning and Refrigeration Center, 2003.

[3] R. Zhou, T. Zhang, J. Catano, J. T. Wen, G. J. Michna, and Y. Peles, "The steady-state modeling and optimization of a refrigeration system for high heat flux removal," *Applied Thermal Engineering*, vol. 30, pp. 2347–2356, 2010.

[4] T. Hovgaard, L. Larsen, M. Skovrup, and J. Jørgensen, "Optimal energy consumption in refrigeration systems - modeling and non-convex optimization," *The Canadian Journal of Chemical Engineering*, vol. 9999, 2012.

[5] L. N. Petersen, H. Madsen, and C. Heerup, "Eso2 optimization of supermarket refrigeration systems," tech. rep., Technical University of Denmark, Department of Informatics and Mathematical Modeling, 2012.

[6] D. Sarabia, F. Capraro, L. F. S. Larsen, and C. Prada, "Hybrid nmpc of supermarket display cases," *Control Engineering Practice*, vol. 17, pp. 428–441, 2009.

[7] C. Pérez-Segarra, J. Rigola, M. Sòria, and A. Oliva, "Detailed thermodynamic characterization of hermetic reciprocating compressors," *International Journal of Refrigeration*, vol. 28, pp. 579–593, 2005.

[8] J. M. Yin, C. W. Bullard, and P. S. Hrnjak, "R744 gas cooler model development and validation," tech. rep., University of Illinois, Air Conditioning and Refrigeration Center, 2000.

[9] M. Corradi, L. Cecchinato, and G. Schiochet, "Modeling fin-and-tube gas-cooler for transcritical carbon dioxide cycles," in *International Refrigeration and Air Conditioning Conference*, (Lafayette, Indiana, USA), 2006.

[10] Y. Ge and R. Cropper, "Simulation and performance evaluation of finned-tube co_2 gas cooler for refrigeration systems," *Applied Thermal Engineering*, vol. 29, pp. 957–965, 2009.

[11] L. Ljung, "Prediction error estimation methods," *Circuits, Systems, and Signal Processing*, vol. 21, no. 1, pp. 11–21, 2002.

[12] M. J. Skovrup, *Thermodynamic and Thermophysical Properties of Refrigerants, Version 3.00*. Technical University of Denmark, 2000.